DOI: 10.53375/ijecer.2022.312

A Compact MIMO Antenna for UWB Applications

María del Carmen Hernández-Serrano[1], Gabriela Leija-Hernández[2], Luis Alejandro Iturri-Hinojosa[3,*]

[1]Instituto Politécnico Nacional ESIME Zacatenco C.P.07320, Ciudad de Mexico, México,
Email: mcarmen.hs.acc@gmail.com

[2]Instituto Politécnico Nacional ESIME Zacatenco C.P.07320, Ciudad de Mexico, México,
Email: gleijah5@gmail.com

[3]Instituto Politécnico Nacional ESIME Zacatenco C.P.07320, Ciudad de Mexico, México,
Email: aiturri@ipn.mx

[*] *Corresponding author*

Abstract: **A 2x1 compact UWB-MIMO antenna with two -10 dB impedance bandwidths of 2.6 GHz and 8.85 GHz is presented. The MIMO antenna dimension is 5.3 cm × 3.8 cm and is composed by two symmetrical rectangular patches, each one with a resonance frequency at 4 GHz. An EBG structure is introduced between the elements to increase de isolation and improve the MIMO antenna performance. The transmission coefficient of the MIMO antenna with EBG structure reaches a minimum of -28.9 dB at 8.18 GHz, and its maximum is -16.1 dB at 9.9 GHz. The impedance bandwidth is 5.9 GHz, and the maximum gain of the proposed antenna is 6 dBi.**

Keywords: **2x1 compact antenna, EBG, MIMO antenna, UWB**

I. INTRODUCTION

The Federal Communications Commission (FCC) defines a very wide frequency band (3.1 GHz – 10 GHz) for UWB (Ultra-Wideband) systems and a signal bandwidth greater than or equal to 500 MHz. UWB wireless systems are characterized by their high bandwidth, high bit rate, high energy efficiency, and their very low nominal transmission power for short-distance applications [1-3]. Due to this type of application, UWB systems suffer from multipath fading, which is solved by incorporating multiple input multiple output (MIMO) technology. Likewise, extremely wideband indoor transmission causes interference with other narrowband technologies if the power spectral density of the UWB signal exceeds -41.3 dBm [3,4]. With the implementation of MIMO technology, multipath propagation is confronted thanks to the simultaneous operation of several transmitting and receiving antennas, giving the system high data transmission, allowing multiple users to access several services at the same time [5]. In this way, UWB systems with MIMO antenna arrays are characterized by their low equipment cost, wide bandwidth, simple structure, multipath immunity, increased diversity, and multiplexing [6].

In a compact antenna array, a higher energy coupling occurs mainly due to the proximity of the elements. A high mutual coupling degrades radiation characteristics and the system performance significantly. For example, the signal-to-interference ratio (SINR) decreases, as does the convergence of array algorithms and radar cross section (RCS) [7-9]. So, the challenges for the designers are the conditioning in reduced spaces, and the proper design of user terminals and base stations. The design of a MIMO antenna should search for an isolation less than -15 dB [5].

Some techniques have been developed to increase the isolation between the elements of a MIMO array antenna, such as the implementation of an EBG (Electromagnetic Bandgap) structure that acts as a band rejection filter [10], parasitic element slots [10,11], defected ground structures (DGS) [12,13], and perforated ground planes. Some proposals are described below.

In [14] a MIMO antenna for a fifth generation (5G) system operating at the 3.5 GHz frequency is presented. The array elements are perforated rectangular patches. The array antenna reaches a return loss equal to -25 dB with a bandwidth of 220 MHz and the isolation coefficient obtained is -70 dB. The gain of the proposed antenna is 10 dB.

An EBG structure implemented in a dual polarized MIMO antenna is presented in [15]. The EBG consists of periodical cells of dielectric elements. The bandwidth of the proposed antenna is from 5.70 to 5.93 GHz, reaches a peak gain of 5.45 dBi, with a maximum isolation of -20 dB.

A uniplanar mushroom-like EBG structure decoupling network in a UWB-MIMO arrangement of two semicircular staggered monopoles angularly separated by 90 degrees is proposed by [16]. The proposed antenna achieves isolation greater than 15 dB and its application is for WiMAX, WLAN and X-Band satellite downlink communication.

The MIMO antenna proposed in [17] has two radiation patches with an EBG structure between the elements and a rectangular ground plane. The effect of implementing an EBG structure is a reduction of mutual coupling up to -30 dB, in the frequency band 2.2 to 3.6 GHz and 5.5 to 5.9 GHz.

A double-sided MIMO array with a decoupling structure for UWB applications is presented in [18]. The MIMO antenna with four square elements achieves a large bandwidth of 7.7 GHz from 3.3 GHz to 11 GHz, with an average gain of 4.36 dBi. Each element has a similar shape to the square patch element of the MIMO antenna present here.

This paper presents the implementation of an EBG structure in a 2x1 MIMO antenna array, located between the two microstrip elements. The simulation of the MIMO antenna is performed with the help of the Ansoft HFSS software. The geometry of the EBG structure was optimized to reduce the mutual coupling between the elements and therefore enhance the performance application.

II. RECTANGULAR PATCH ANTENNA DESIGN

The microstrip-line feed antenna is printed on FR4 epoxy dielectric substrate with a 4.4 dielectric constant (ε_r), thickness of 1.6 mm (h), loss tangent of 0.02 and is initially designed for the resonant frequency of 7 GHz.

The patch has a length L_p and a width W_p, and is printed over the dielectric substrate. The width and length of the ground plane are $W_g(=W+10h)$ and $L_g(=L_p-2*x_0+2*L_f)$, respectively, and is printed on the other side of the substrate. The analytical expressions used for the rectangular microstrip line feed design are presented in [19]. Fig. 1 shows the rectangular microstrip geometry.

The patch width W_p is given by:

$$W=\frac{\lambda_o}{2}\sqrt{\frac{2}{\varepsilon_r+1}} \tag{1}$$

where $\lambda_o(\lambda_o=c/f)$ is the operating signal wavelength.

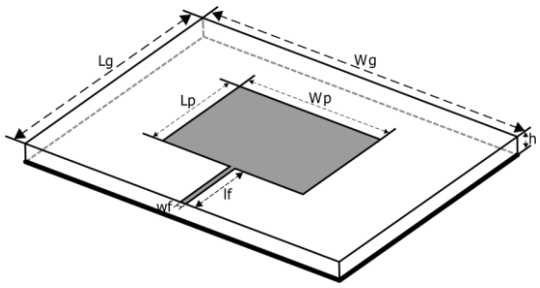

Fig. 1. Microstrip antenna geometry.

The effective dielectric constant is obtained with (2).

$$\varepsilon_{\varepsilon ff}=\frac{\varepsilon_r+1}{2}+\frac{\varepsilon_r-1}{2}\left(\frac{1}{\sqrt{1+\frac{10h}{W}}}\right) \tag{2}$$

The incremental length (ΔL) for fringing field can be calculated with (3).

$$\Delta L=0.412h\left[\frac{\varepsilon_{eff}+0.3}{\varepsilon_{eff}-0.258}\right]\left[\frac{\frac{W}{h}+0.264}{\frac{W}{h}+0.813}\right] \tag{3}$$

For the TM_{010} dominant mode without radiation fringes, considering the wavelength in the substrate (λ_g), the patch length (L) is equal to $\frac{\lambda_g}{2}$, where $\lambda_g=\frac{\lambda_o}{\sqrt{\varepsilon_{eff}}}$.

By considering the radiation fringes the patch length is given by

$$L=\frac{\lambda_g}{2}-2\Delta L \tag{4}$$

The effective length of the patch is calculated with (5).

$$L_{eff}=L+2\Delta L \tag{5}$$

The resonant frequency (f_r) of the antenna element is calculated using (6).

$$f_r=\frac{1}{2\sqrt{\mu_0\varepsilon_0}L_{eff}\sqrt{\varepsilon_{ef}}} \tag{6}$$

where μ_0 and ε_0 are the vacuum permeability and permittivity.

The patch antenna has an orthogonal radiation respect to the ground plane. The radiated electric field pattern is obtained using (7) to (9) [19].

$$E_\varphi^t=+j\frac{k_0hWE_0e^{-jk_0r}}{\pi r}\left\{\sin\theta\frac{\sin(X)}{X}\frac{\sin(Z)}{Z}\right\}\bullet$$
$$\bullet\cos\left(\frac{k_0L_e}{2}\sin\theta\sin\varphi\right) \tag{7}$$

$$X=\frac{k_0h}{2}\sin\theta\cos\varphi \tag{8}$$

$$Z=\frac{k_0W}{2}\cos\theta \tag{9}$$

The line feed is characterized by a length (l_f), a width (w_f) and a Z_f impedance and connect the patch with the SMA connector that has a $Z_2(=50\Omega)$ impedance. The patch impedance is calculated with (10).

$$Z_p=\frac{90\varepsilon_r^2}{\varepsilon_r-1}\left(\frac{L}{W}\right)^2 \tag{10}$$

The line feed impedance is calculated with (11).

$$Z_f=\sqrt{Z_pZ_2} \tag{11}$$

The line feed length (l_f) in millimeters is calculated with (12).

$$l_f=\frac{\theta_{a,rad}}{k_0\sqrt{e}} \tag{12}$$

where $\theta_{a,rad}(=\pi/2)$ is the length of the coupling transmission line of quarter wavelength ($\lambda/4$) and e is calculated with (13).

$$e = 0.5(\varepsilon_r + 1) \frac{0.5(\varepsilon_r - 1)}{\sqrt{1 + 12\frac{h}{W_0}}} \quad (13)$$

where $W_o = W_d \cdot h$, for which $W_d = W_{d1}$ if $W_{d1} < 2$, either $W_d = W_{d2}$ if $W_{d1} \geq 2$. And

$$W_{d1} = \frac{8e^A}{e^{2A} - 2} \quad (14)$$

$$W_{d2} = \frac{2}{\pi}\left\{ B - 1 - \ln(2 * B - 1) + \frac{\frac{\varepsilon_r - 1}{2}}{\varepsilon_r} * \right.$$

$$\left. * \left(\ln(B - 1) + 0.39 - \frac{0.61}{\varepsilon_r} \right) \right\} \quad (15)$$

With:

$$A = \frac{z_0}{60} * \sqrt{0.5 * (\varepsilon_r + 1)} + \frac{\varepsilon_r - 1}{\varepsilon_r + 1}\left(0.23 + \frac{0.11}{\varepsilon_r} \right) \quad (16)$$

$$B = 377 * \frac{\pi}{2 * z_0 * \sqrt{\varepsilon_r}} \quad (17)$$

With the above equations, the geometric parameters for the inset-feed patch antenna at 4 GHz are given in Table I. The wavelength is equal to 75 mm, the effective dielectric constant ($\varepsilon_{\varepsilon ff}$) results equal to 3.9528, the incremental length (ΔL) is 0.731 mm, the patch impedance (Z_p) and the line feed impedance (Z_f) are equal to 297.87 Ω and 122.04 Ω, respectively.

In the antenna element, the ground plane size (w_g, l_g) is the same of the dielectric substrate.

TABLE I. GEOMETRIC PARAMETERS OF THE PATCH ANTENNA ELEMENT

Parameter	Value, mm
W_p	22.82
L_p	17.39
W_s	38.00
L_s	40.00
l_f	10.94
w_f	0.396

III. PATCH ANTENNA ELEMENT

Some geometric dimensions were optimized to achieve a compact antenna geometry and a larger operating bandwidth.

The performance optimization consists in increasing the patch size, width (W_p) and large (L_p), the dielectric substrate width (W_g), the line feeder width (W_f) in multiples of 0.2 mm. At the same time, the ground plane has been reduced to 0.07λ and increased in multiples of 0.2 mm until a minimum return loss response is achieved at the resonant frequency of 4 GHz. Fig. 2 shows the rectangular patch antenna with optimized dimensions.

A full-wave simulation of the proposed antenna is conducted with ANSYS High Frequency Structural Simulator (HFSS).

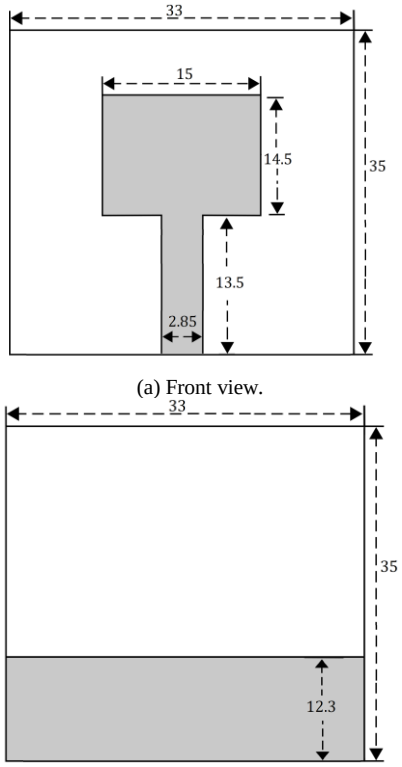

(a) Front view.

(b) Back view.

Fig. 2. Patch antenna geometry. Units in millimetres.

Fig. 3 presents the return loss response for different sizes of the ground plane (l_g), keeping its width (w_g) equal to that of the dielectric substrate. A 12.3 mm is considered as the adequate length of the ground plane to achieve the highest operating bandwidth and a peak gain equal to 1.71 dB in the H-plane radiation, and 2.36 dB in the E-plane radiation.

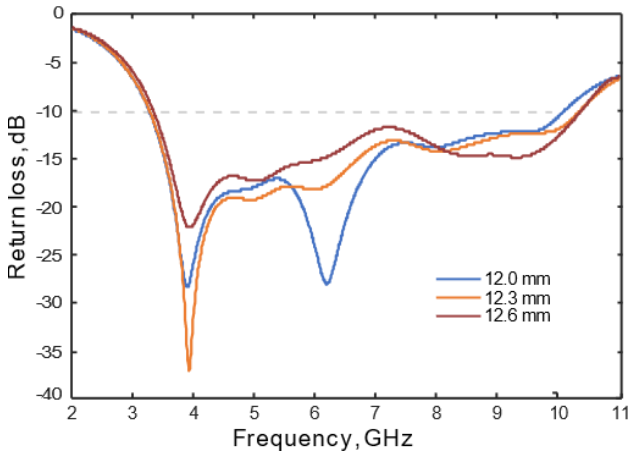

Fig. 3. Simulated return loss for different larges of ground plane.

Fig. 4 shows the return loss comparison of the patch antenna with non-optimized dimensions from Table I with that of the patch antenna with optimized dimensions of Fig. 2.

The optimized patch antenna has an operating frequency band of 7.1 GHz, from 3.3 GHz to 10.4 GHz. The resonance frequency of the antenna is equal to 3.93 GHz, with a return loss value of -40.8 dB and a maximum gain of 2.36 dB.

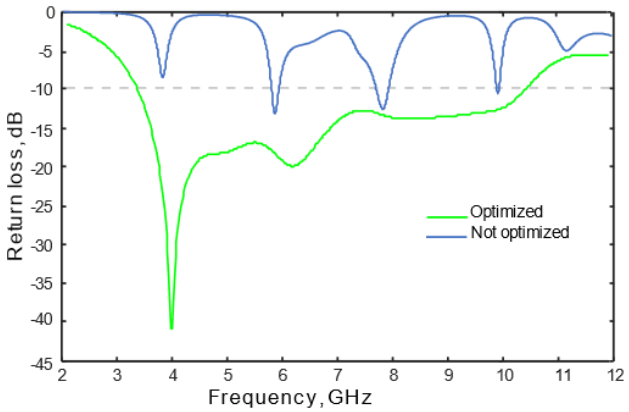

Fig. 4. Simulated return loss for the optimized geometry.

IV. THE 2X1 MIMO ANTENNA

Two rectangular patch antennas of Fig. 2 are placed side to side, spaced 6.5 millimetres, to conform the MIMO antenna. The compact 2x1 MIMO antenna is 20.14 cm^2 (5.3 cm × 3.8 cm). The antenna geometry is shown in Fig. 5.

Simulated results of reflection (S_{11}) and transmission (S_{21}) coefficients are presented in Fig. 6.

There exist three operating bandwidths, 1.63 GHz (2.96 GHz to 4.59 GHz), 1.95 GHz (4.97 GHz to 6.92 GHz) and 3.07 GHz (7.33 GHz to 10.4 GHz), as shown in Fig. 6. A resonant frequency is observed at 3.67 GHz with reflection coefficients of -30.1 dB.

There is a strong electromagnetic coupling between the radiating patches since the transmission coefficient (S_{21}) is between -10.4 dB and -22.4 dB at the bandwidth from 2.96 GHz to 10.4 GHz.

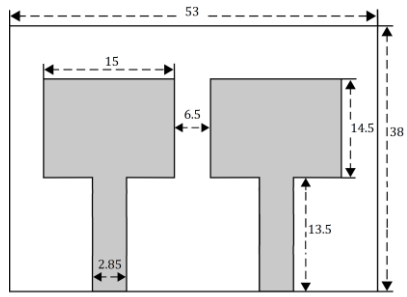

(a) Top view.

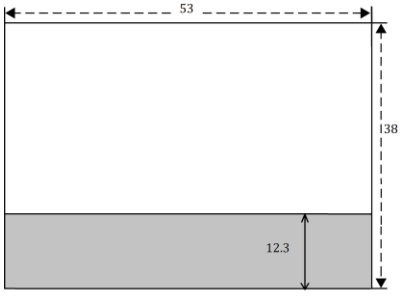

(b) Back view.

Fig. 5. Geometry of the compact 2x1 MIMO antenna. Units in millimeters.

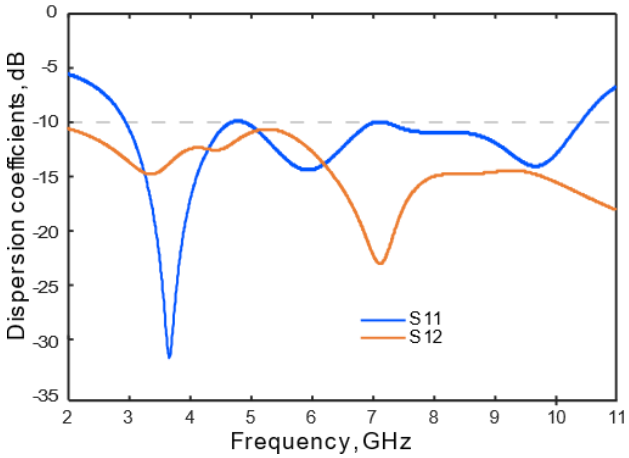

Fig. 6. S parameters of the 2x1 MIMO array antenna.

V. THE MIMO ANTENNA WITH EBG STRUCTURE

Good isolation between closely spaced antennas is required for MIMO communication systems. To improve the isolation, an Electromagnetic Band Gap (EBG) structure is designed and introduced between the antenna elements. Below, the methodology used for the design of the EBG structure is presented. The design of the EBG structure begins by adding a vertical microstrip of width w_v in the centre of the ground plane. Fig. 7 presents the reflection and transmission coefficient responses of the MIMO antenna with 3 widths of the added microstrip. The geometry of the MIMO antenna that achieves the greatest bandwidth is the one with the 2 mm wide vertical microstrip.

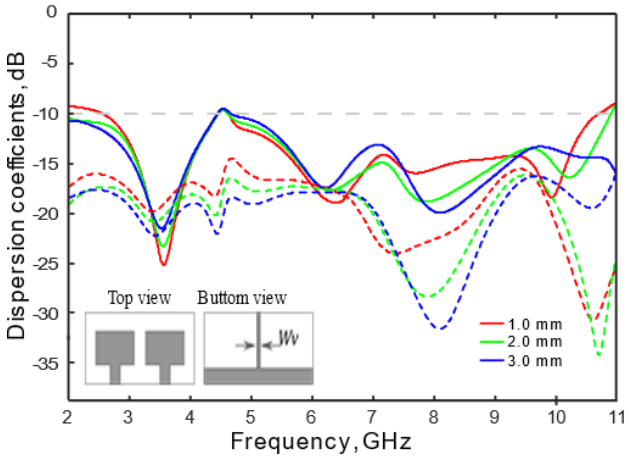

Fig. 7. MIMO antena with a vertical microstrip in ground plane with different widths w_v.

To the above MIMO antenna is added a row of 9x1 vertical square microstrips connected to each other by a microstrip of width 0.7 mm. Each square patch element has a side dimension a. Fig. 8 presents the return loss response of MIMO antennas with values of 1.5, 2.0 and 2.5 millimetres for the dimension a. The MIMO antenna with the widest bandwidth is the one with 2 mm × 2 mm square microstrips as the EBG structure. The transmission coefficient is below -15 dB in the operating bandwidth.

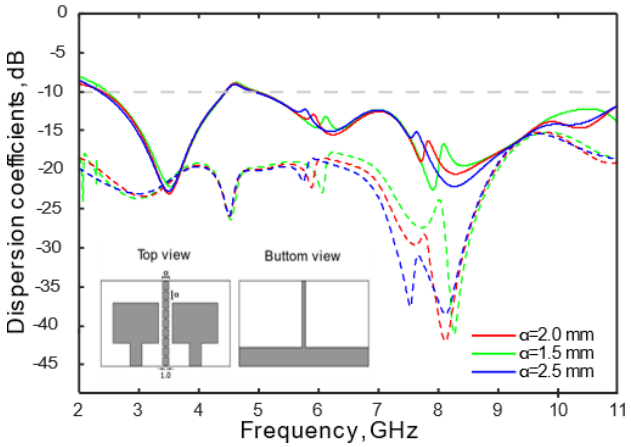

Fig. 8. Dispersion coefficients for MIMO antennas with square patches connected with different microstrip widths.

The 9x1 periodic metal patches (2 mm × 2 mm) on top of the substrate connected with a 0.7mm width microstrip, has vertical viases connecting the square patches to the ground plane. The purpose of connected the decoupling structure to the ground is to neutralize the surface current and increase the gain of the antenna [17].

The compact 2x1 MIMO antenna dimension with EBG structure is 53 mm x 38 mm and is given in Fig. 9. The MIMO antenna with the EBG structure has a transmission coefficient of -23 dB and -29 dB at 3.50 GHz and 8.18 GHz, respectively.

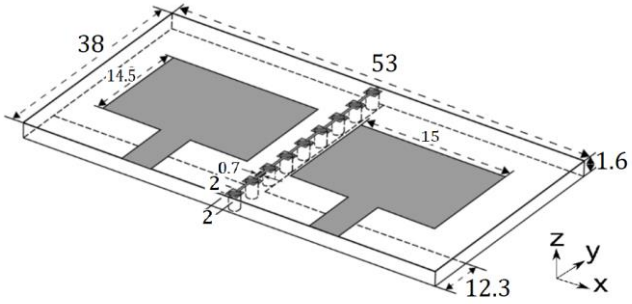

Fig. 9. The compact 2x1 MIMO antenna with EBG structure. Units in millimeters.

The reflection (S_{11}) and transmission ($S_{12}=S_{21}$) coefficients obtained by simulation are shown in Fig. 10.

Fig. 11 shows the simulated far-field radiation patterns of the proposed UWB-MIMO antenna for E-plane and H-plane at the two operating bandwidths. In the E-plane radiation the maximum gain is 4.30 dB in $\theta=50^{o}$ and $\theta=-95^{o}$ at the frequencies 8.18 GHz and 3.5 GHz. In the H-plane radiation the maximum gains are 6.5 dB ($\varphi=135^{o}$) and 6.0 dB ($\varphi=105^{o}$) at the frequencies 8.18 GHz and 3.5 GHz, respectively.

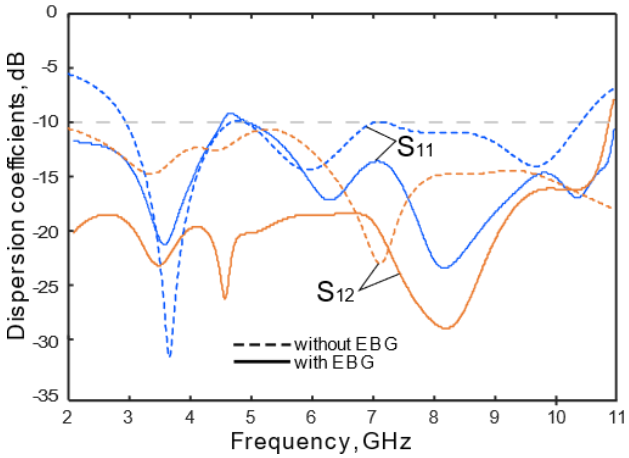

Fig. 10. S parameters of the MIMO antenna with and without the EBG structure.

The return loss response at the frequency band from 4.46 GHz to 4.90 GHz is greater than -10 dB. All frequencies outside of this band will have at least 90% of the power and will be radiated by the antenna.

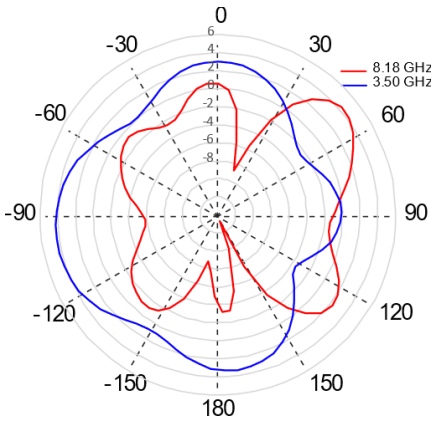

(a) E-plane ($\phi = 0^{o}$).

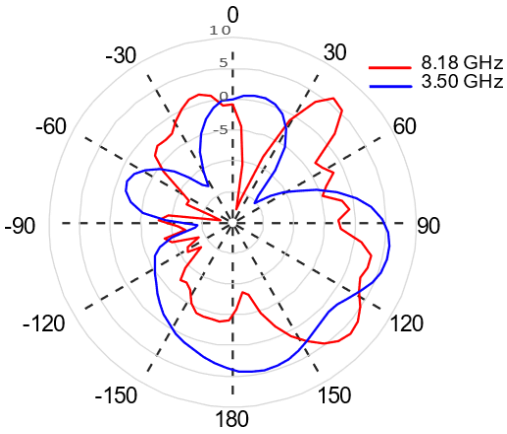

(b) H-plane ($\theta = 90^{o}$).

Fig. 11. Normalized radiation patterns of the proposed MIMO antenna. S parameters of the MIMO antenna with and without the EBG structure.

VI. CONCLUSIONS

A 2x1 compact UWB-MIMO antenna with -10 dB impedance bandwidth from 1.86 GHz to 4.46 GHz and from 4.9 GHz to 10.75 GHz is presented. An EBG structure is introduced between the elements to increase de isolation and improve the MIMO antenna performance. With the EBG structure the isolation is less than -18.5 dB in the first frequency band, and less than -16 dB in the second. The MIMO antenna geometry is 20.14 cm^2 (5.3 cm × 3.8 cm) and is composed by two symmetrical rectangular patches, each one with a resonance frequency at 4 GHz. The transmission coefficient of the MIMO antenna with EBG structure reaches a minimum of -28.9 dB at 8.18 GHz, and its maximum is -16.1 dB at 9.9 GHz. A high isolation in the two frequency bands is achieved by using the EBG structure. The maximum gain of the proposed antenna is 6 dBi. Simulated results of S-parameters and radiation patterns are presented.

ACKNOWLEDGMENT

The authors express thanks to the support received by the project SIP20221930.

REFERENCES

[1] P. Kumar, et al., "Design of a Six-Port Compact UWB MIMO Antenna with a Distinctive DGS for Improved Isolation," *IEEE Access*, vol. 10, pp. 112964-112974, 2022.

[2] M. G. N. Alsath and M. Kanagasabai, "Compact UWB monopole antenna for automotive communications," *IEEE Transactions on Antennas and Propagation*, vol. 63, no. 9, pp. 4204–4208, 2015.

[3] B. Wang, H. Song, W. Rhee and Z. Wang, "Overview of ultra-wideband transceivers—system architectures and applications," *Tsinghua Science and Technology*, vol. 27, no 3, pp. 481-494, 2021.

[4] G. Breed, "A summary of FCC rules for ultra wideband communications," *High Frequency Electronics*, vol. 4, no 1, pp. 42-44, 2005.

[5] A. K. Gautam, S. Yadav and K. Rambabu, "Design of ultra-compact UWB antenna with band-notched characteristics for MIMO applications," *IET Microwaves, Antennas & Propagation*, vol. 12, no 12, pp. 1895-1900, 2018.

[6] J. Jervase-Yak, "MIMO antenna for uwb communications," *International Journal of Communications, Network and System Sciences*, vol. 9, no 05, pp. 177, 2016.

[7] M. El Ouahabi, A. Dkiouak, A. Zakriti, M. Essaaidi and H. Elftouh, "Analysis and design of a compact ultra-wideband antenna with WLAN and X-band satellite notch," *International Journal of Electrical and Computer Engineering*, vol. 10, no 4, pp. 4261, 2020.

[8] H. Singh, H. L. Sneha and R. M. Jha, "Mutual coupling in phased arrays: A review," *International Journal of Antennas and Propagation*, vol. 2013, 2013.

[9] C. Abdelhamid, H. Sakli, and N. Sakli, "A four-element UWB MIMO antenna using SRRs for application in satellite communications," *International Journal of Electrical and Computer Engineering*, vol. 11, no 4, pp. 3154, 2021.

[10] A. C. K. Mak, C. R. Rowell and R. D. Murch, "Isolation enhancement between two closely packed antennas," *IEEE Trans Antennas Propagation*, vol. 56, no 11, pp. 3411-3419, 2008.

[11] X. Sun and M. Cao, "Mutual coupling reduction in an antenna array by using two parasitic microstrips," *AEU-International Journal of Electronics and Communications*, vol. 74, pp. 1-4, 2017.

[12] M. S. Sharawi, M. U. Khan, A. B. Numan and D. N. Aloi, "A CSRR loaded MIMO antenna system for ISM band operation," *IEEE Transactions on antennas and propagation*, vol. 61, no 8, pp. 4265-4274, 2013.

[13] F. G. Zhu, J. D. Xu and Q. Xu, "Reduction of mutual coupling between closely-packed antenna elements using defected ground structure," *IEEE International Symposium on Microwave, Antenna, Propagation and EMC Technologies for Wireless Communications*, IEEE, pp. 1-4, 2009.

[14] F. Solehudin, Z. A. Sanaz, S. Alam, L. Sari and I. Surjati, "Design of 2x1 MIMO Microstrip Antenna Using Slit and Inset Technique For 5G Communication," *JOURNAL OF INFORMATICS AND TELECOMMUNICATION ENGINEERING*, vol. 5, no 1, pp. 31-44, 2021.

[15] X. Y. Zhang, X. Zhong, B. Li and Y. Yu, "A dual-polarized MIMO antenna with EBG for 5.8 GHz WLAN application," *Progress In Electromagnetics Research Letters*, vol. 51, pp. 15-20, 2015.

[16] N. Jaglan, et al., "Triple band notched mushroom and uniplanar EBG structures based UWB MIMO/Diversity antenna with enhanced wide band isolation," *AEU-International Journal of Electronics and Communications*, vol. 90, pp. 36-44, 2018.

[17] P. Beigi, M. Rezvani, Y. Zehforoosh, J. Nourinia and B. Heydarpanah, "A tiny EBG-based structure multiband MIMO antenna with high isolation for LTE/WLAN and C/X bands applications" *International Journal of RF and Microwave Computer-Aided Engineering*, vol. 30, no 3, pp. e22104, 2020.

[18] M. A. Hasin, M. T. Ali, H. Yong, B. Baharom and H. Jumaat, "Development of MIMO antenna with decoupling structure for ultra-wideband application," *Indonesian Journal of Electrical Engineering and Computer Science*, vol. 16, no. 2, pp. 818-826, 2019.

[19] C. A. Balanis, "Antenna theory: analysis and design," *John wiley and sons*, 2015.